Surface x-ray-absorption fine structures of SiO_x $(0<x<2)$ and SiN_x $(0<x<4/3)$ produced by low-energy ion implantation in Si(100)

Y. Baba, H. Yamamoto, and T. A. Sasaki
Advanced Science Research Center, Japan Atomic Energy Research Institute, Tokai-mura, Naka-gun, Ibaraki-ken, 319-11, Japan
(Received 10 February 1993)

X-ray-absorption near-edge structures (XANES) have been investigated for silicon oxide and nitride with nonstoichiometric compositions (SiO_x, SiN_x) produced by low-energy ion implantation in Si(100). The XANES structures at the Si $2p$ edge for SiO_x at $x \geq 0.2$ resemble those reported for SiO_2, and those at the O $1s$ edge are independent of the x value. These observations indicate that the conduction band of SiO_x is mainly composed of the orbitals of SiO_2. On the other hand, the XANES structures of SiN_x change with the x value, and the sharp resonance corresponding to a N dangling bond was observed at the N $1s$ edge for $x > 1.0$. These findings suggest that in the SiN_x phase there is a random-bonding structure rather than a mixture of Si and Si_3N_4 islands.

I. INTRODUCTION

Silicon dioxide (SiO_2) and silicon nitride (Si_3N_4) are widely used for microelectronic devices such as passivation layers and insulating layers in thin-film transistors.[1-6] As well as such stoichiometric compounds, the electronic structures of compounds with nonstoichiometric composition, i.e., SiO_x $(0<x<2)$ and SiN_x $(0<x<\frac{4}{3})$, are of great importance, since these layers in the interface between the semiconductor and insulator influence the electric properties in the circuit, especially in very large scale integrated electronics.

The electronic structures of nonstoichiometric silicon compounds have been investigated for SiO_x (Refs. 7–17) and SiN_x (Refs. 17 and 18) by means of photoelectron spectroscopy. These methods provide information about the electronic structures of occupied orbitals. Although many of the electrical properties depend on the electronic structures in the conduction-band region, the unoccupied states of such nonstoichiometric silicon compounds have not been fully understood. In the present work, the technique of x-ray-absorption near-edge structure (XANES) is applied to elucidate the electronic structures of unoccupied orbitals for SiO_x and SiN_x to learn the conduction-band structures.

XANES is useful for elucidation of the conduction-band structures because it provides information about electronic transitions from the core to the unoccupied states, if we adopt a one-electron transition (or single-particle) approximation. In addition, XANES is sensitive to the orbitals surrounding the atom whose core level is being measured. This implies that we can learn the electronic structure of both silicon and oxygen (or nitrogen) sites separately by adjusting the incident photon energy to each core level.

In the present paper, XANES at Si $2p$, Si $2s$, and O $1s$ (or N $1s$) absorption edges are measured for SiO_x and SiN_x layers, which were produced by ion implantation. X-ray photoemission spectroscopy (XPS) is also measured as a reference to learn the electronic structures of the occupied orbitals in the core region.

II. EXPERIMENT

The target material used was a Si(100) single crystal of high-purity grade (>99.9999 at. %). The surface of the sample was mechanically polished with a diamond paste of $\frac{1}{4}$ μm, and then cleaned in vacuum by repeating the 3-keV Ar^+ sputtering and 800 °C annealing.

XANES measurements and ion implantation were performed in the same vacuum chamber with a base pressure of 3×10^{-7} Pa. An ion gun of a Penning-ion gauge (PIG) type was used for the ion implantation. High-purity oxygen and nitrogen gases were used for the production of O_2^+ and N_2^+ ions, respectively. The accelerating voltage of the molecular ions was 10 keV, which corresponds to 5-keV atomic ions. The incident angle of the ion beam was 25° from the surface normal. The pressure during the bombardment was kept at 1×10^{-4} Pa. It was checked that the ion-assisted trapping of atmospheric gases[19,20] does not occur at this pressure. The beam current was fixed to be 2 $\mu A/cm^2$ (2.5×10^{13} atoms/cm^2 s).

XANES measurements were performed at the Grasshopper Monochromator Station BL-11A of the Photon Factory in the National Laboratory for High-Energy Physics (KEK-PF). XANES spectra were taken after ion implantation by recording the total electron yield (TEY) as a function of photon energy. The TEY was normalized to the photon intensity which was measured by a copper mesh located in front of the sample. The polar angle of the electric vector of incident x rays was fixed to be 90°. As a detector of secondary electrons, a channeltron was used, and it was located at a 45° direction from the sample surface.

XPS was also measured with another UHV chamber, which has been described elsewhere.[15-17] This instrument was also equipped with an ion-implantation system.

The experimental conditions of the sample preparation and ion implantation were the same as those for the XANES measurements. An Al $K\alpha$ (1486.6 eV) x ray was used as an excitation source, and the peak energy was calibrated such that the Au $4f_{7/2}$ line of metallic gold was 84.0 eV. The Auger spectra were also taken during the XPS measurements (x-ray-induced Auger electron spectra, XAES).

III. RESULTS AND DISCUSSION

A. SiO_x

Figure 1 shows the TEY at the Si $2p$ and Si $2s$ edges as a function of photon energy for SiO_x at various ion doses (hereafter we call these curves the XANES spectrum). In Fig. 2, the XANES spectra at the O $1s$ edge for SiO_x are displayed. In both figures, the surface O/Si ratio (x) determined by the peak areas of XPS is indicated in each figure. For comparison, the electronic structures in occupied core orbitals were also measured. The results for the Si $2p$ XPS and Si_{KLL} XAES for the same samples are also indicated in Figs. 3 and 4, respectively.

In Fig. 1, the XANES spectrum before ion implantation [clean surface of Si(100)] is similar to the previously

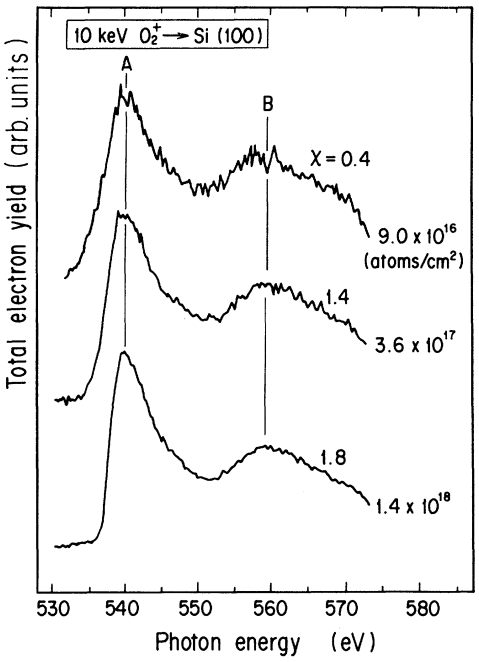

FIG. 2. XANES spectra at the O $1s$ edge for O_2^+-implanted Si(100) at various ion fluences.

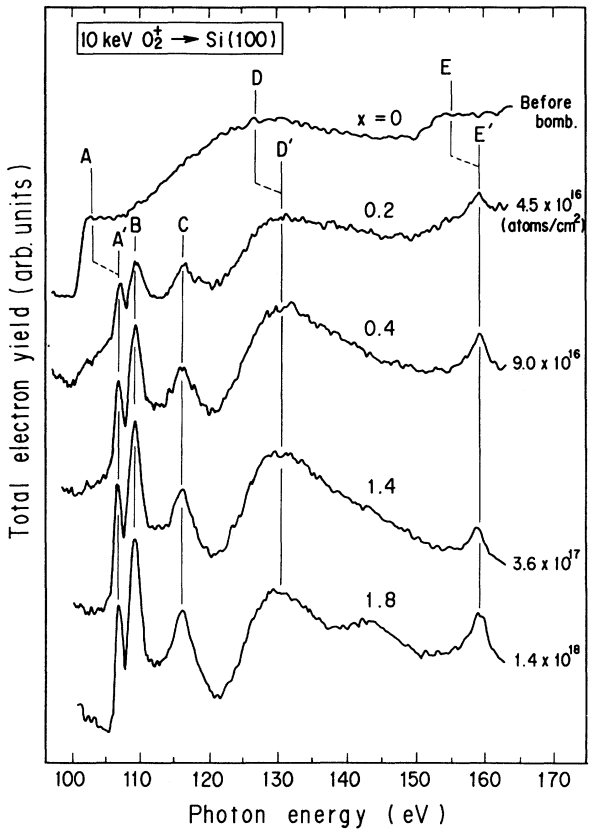

FIG. 1. XANES spectra at Si $2p$ and Si $2s$ edges for O_2^+-implanted Si(100) at various ion fluences. The surface O/Si ratio determined by XPS is indicated as x in each spectrum.

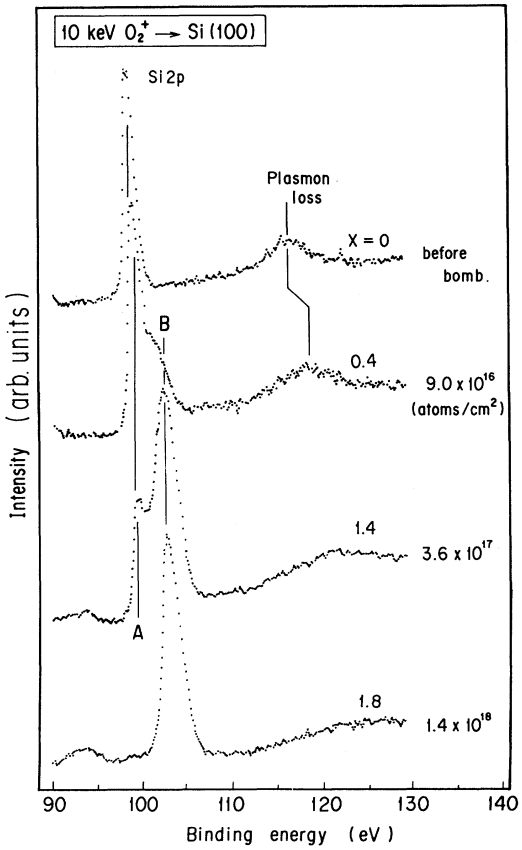

FIG. 3. Si $2p$ XPS for O_2^+-implanted Si(100) at various ion fluences.

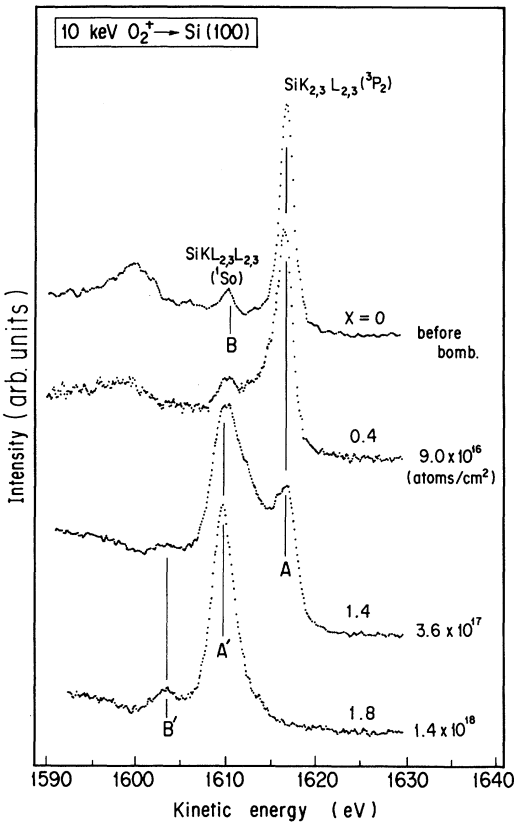

FIG. 4. Si_{KLL} XAES for O_2^+-implanted Si(100) at various ion fluences.

reported x-ray-absorption fine structures for silicon.[21–29] In the case of pure atomic silicon, the surrounding crystal environment is little perturbed. Thus it is assumed that only dipole-allowed transitions are observed in the XANES spectrum. Therefore, peaks A and D are assigned to the Si $2p \rightarrow a_1(3s)$ and Si $2p \rightarrow t_2 + e(\epsilon d)$ transitions, respectively. Peak E is assigned to the transition from Si $2s$ to the $3d$-derived state.

XANES spectra of SiO_x produced by the O_2^+-ion implantation are quite similar to those reported for bulk SiO_2 or an oxide overlayer produced by the thermal oxidation of silicon.[21,24–29] The intensity of peak A of the pure silicon immediately decreases at $x = 0.2$, and the peak almost disappears at $x = 0.4$.

We note that peak A shifts to the higher-energy side (A') for the spectra of $x \geq 0.2$, which is based on the Si $2p$ XPS spectra (see Fig. 3). Although the Si $2p$ peak is slightly broadened with increasing x, the peak for SiO_x apparently consists of two components, i.e., a 99.5-eV peak of pure Si (peak A) and a 102.8-eV peak corresponding to SiO_2 (peak B). Such a two-phase structure for SiO_x is more clearly observed in the Si_{KLL}-XAES spectra (Fig. 4) because of the large chemical shift between Si and SiO_2.

In the Si $2p$ XPS, the energy separation of two components is 3.3 eV, which is close to that observed in XANES between peaks A and A'. If we ignore the difference of the final-state relaxation effects between XPS and XANES,[30–32] peak A' in XANES can be assigned to the transitions from chemically shifted Si $2p$ to the $\sigma^*(a_1)$ valence orbital.

The shifts to higher energy of 3–4 eV are also observed for peaks D and E. Thus peaks D' and E' also originate from the chemically shifted Si $2p \rightarrow$ Si $3d$ and Si $2s \rightarrow$ Si $3p$-derived state transitions, respectively.

In the case of SiO_2, the tetrahedrally coordinated and strongly electronegative oxygen atoms change the symmetry of the crystal field to enable transitions to the $3p$-derived states.[28] Therefore peak B is assigned to the transition to the $\sigma^*(t_2)$ valence orbital. Structures C and D' are due to the shape resonances in the continuum corresponding to the excitation to t_2 and e orbitals of $3d$ character.[24,25]

On the other hand, XANES spectra at the O $1s$ edge (Fig. 2) scarcely change except for the increase in intensity with x. Peak A at around 540 eV is assigned to the transition from O $1s$ to the Si $3p$-like orbital (generally called the "π-resonance peak"). Peak B above the O $1s$ ionization threshold is assigned to the continuum shape resonance which appears due to the presence of the crystal lattice of the SiO_4 microscopic unit (generally called the "σ-resonance peak"). These two structures also have been observed for oxygen-adsorbed silicon.[31] The constant spectrum shape in Fig. 2 suggests that all the implanted oxygen atoms constitute the SiO_4 unit structure. This finding excludes the possibility that phases other than the SiO_4 unit exist in the oxygen site of the SiO_x phase.

Regarding the microstructure of nonstoichiometric SiO_x, two contradictory models have been proposed. One is the random-mixture model (RMM), in which the SiO_x phase is interpreted as a mixture of Si and SiO_2 regions as small as 0.5–1.0 nm.[33] In this model, silicon atoms are tetrahedrally coordinated to four oxygen atoms to form the SiO_4 unit cell. The remaining region consists of a pure silicon phase. The other is the random-bonding model (RBM), in which each silicon atom is tetrahedrally coordinated to x oxygen and $(4-x)$ silicon atoms with the probability statistically determined.[34] If we adopt the latter model, the absorption peak corresponding to, e.g., the SiO unit would appear in the XANES spectra at the Si $2p$ edge.[25] However, only the structure of the SiO_4 unit is seen in Fig. 1. This result and the two-phase structures in both the Si $2p$-XPS and Si_{KLL}-XAES peaks suggest that the RMM is consistent with the electronic structures of SiO_x compared to the RBM. Regarding the electronic structures of SiO_x, we can conclude that the conduction band of SiO_x at $x \geq 0.2$ is mostly composed of components of the orbitals of SiO_2.

B. SiN_x

Figure 5 displays XANES spectra for the N_2^+-implanted silicon at the Si $2p$ and Si $2s$ edges. XANES spectra at the N $1s$ edge are shown in Fig. 6. The Si $2p$-XPS and Si_{KLL}-XAES spectra for the same sample are presented in Figs. 7 and 8, respectively.

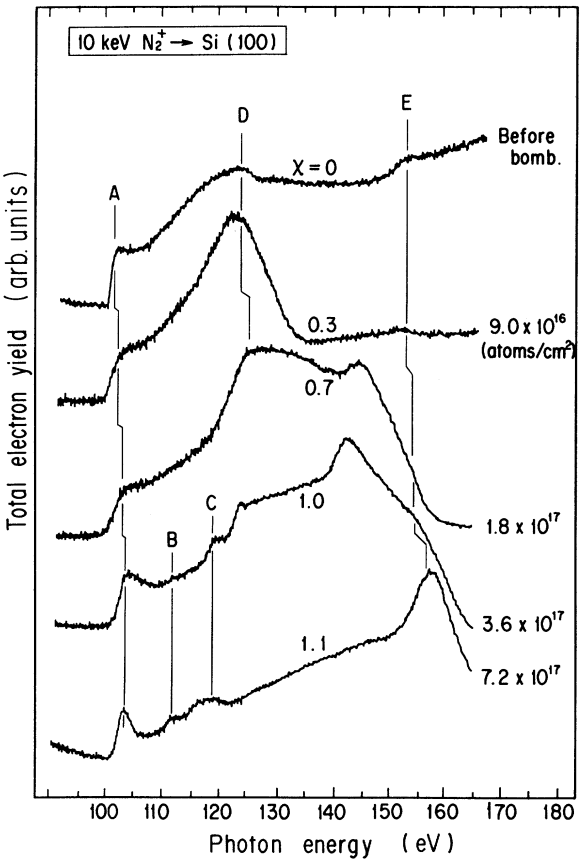

FIG. 5. XANES spectra at Si $2p$ and Si $2s$ edges for N_2^+-implanted Si(100) at various ion fluences. The surface N/Si ratio determined by XPS is indicated as x in each spectrum.

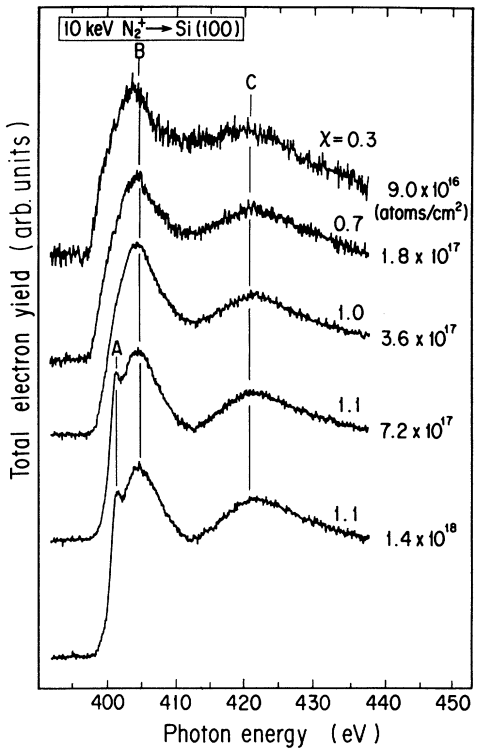

FIG. 6. XANES spectra at the N $1s$ edge for N_2^+-implanted Si(100) at various ion fluences.

In contrast to the SiO_x system, the XANES spectra for SiN_x at the Si $2p$ and Si $2s$ edges (Fig. 5) appreciably change with the x values. Peaks A apparently originate from the Si $2p \rightarrow a_1(3s)$ transition.[27] It should be noted that the peak position of A gradually shifts to higher energy with the x value. This fact is consistent with the Si $2p$ XPS (Fig. 7) and Si_{KLL} XAES (Fig. 8), in which a two-phase structure such as SiO_x is not observed. The gradual energy shifts in the Si $2p$ XPS and Si_{KLL} XAES suggest that there exist several kinds of potentials surrounding the silicon atom. Kärcher, Ley, and Johnson[18] have reported that Si $2p$ XPS of SiN_x produced by dc sputtering consists of five components corresponding to the Si-Si bond replaced by $0 \sim 4$ Si-N bonds. Our results for the XPS are in good agreement with that of Kärcher. Such multicomponent structure is more clearly observed for the Si_{KLL}-XAES spectra (Fig. 8) because of the larger chemical shift in the Auger peak than that in the XPS peak.

The chemically shifted transition is also observed in peaks D and E, which correspond to the Si $2p \rightarrow t_2 + e(\epsilon d)$ and Si $3s \rightarrow$ Si $3p$ transitions, respectively. But the spectral shapes at both edges drastically change with the x values. We assume that these spectral changes are due to the gradual replacement of the Si-Si bond by

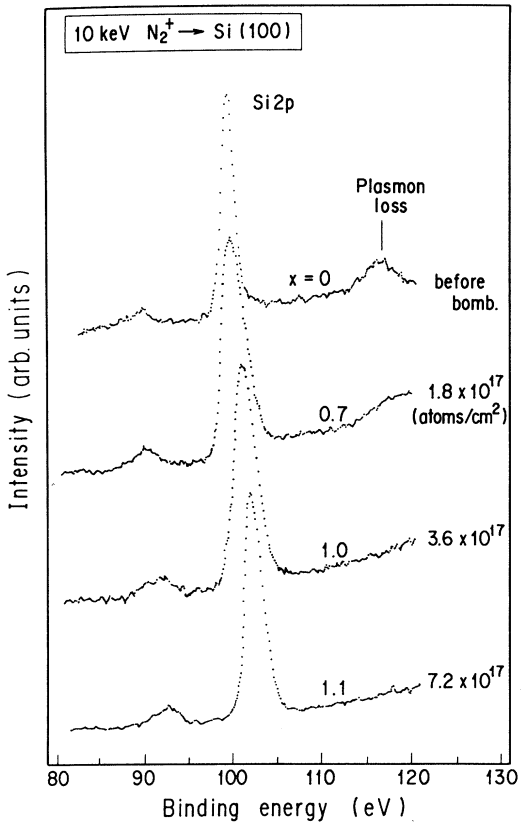

FIG. 7. Si $2p$ XPS for N_2^+-implanted Si(100) at various ion fluences.

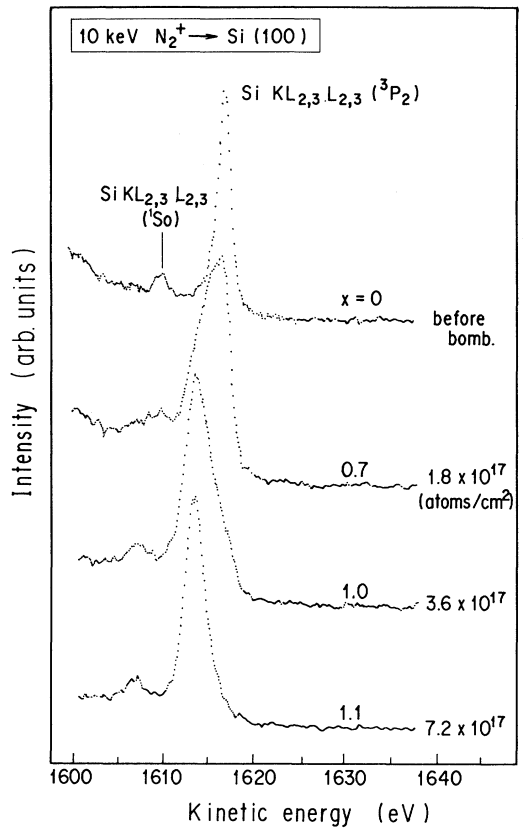

FIG. 8. Si_{KLL}-XAES for N_2^+-implanted Si(100) at various ion fluences.

the Si-N bond.

Filatova, Vinogradov, and Zimkina[27] have demonstrated that the x-ray absorptions corresponding to the Si $2p \rightarrow t_2$ (Si $3p$) and Si $2p \rightarrow e$(Si ϵd) transitions are located at $105 \sim 120$ eV for Si_3N_4. Peaks B and C observed at high fluence ($x \geq 1.0$) might be attributed to these transitions. However, the intensities of these transitions are very weak even at $x = 1.1$. This fact implies that the Si_3N_4 phase of stoichiometric composition is a minor component and each silicon atom is coordinated to nitrogen and silicon atoms with the probability statistically determined.

In the N $1s$-XANES spectra (Fig. 6), a sharp resonance appears at N/Si ≥ 1.1 (peak A). Due to its highly localized p-type character, the line shape is assumed to be attributed to N dangling bonds. Regarding the concentration of the N dangling bonds, it is deduced that the N dangling is a minor component compared with Si-Si and Si-N bonds because the N $2p$ orbitals are highly localized around the nitrogen atom due to its atomiclike character, so that the cross section of this N dangling-bond peak is appreciably higher than those of the other resonance peaks. Such a resonance peak has been observed in XANES for SiN films produced by plasma-enhanced thermal nitridation.[35,36]

It has been reported that the dominant electrical defect in SiN_x is the Si dangling bond.[37] In the present study, such a Si dangling bond could not be detected in the Si-XANES regions (Figs. 1 and 5). The existence of a N dangling bond observed in the N $1s$ XANES may be important in the analysis of the memory-trap mechanism in chemical-vapor-deposition (CVD) memory devices.[38]

IV. CONCLUSIONS

We have measured XANES spectra at the Si $2p$, Si $2s$, O $1s$, and N $1s$ edges for SiO_x and SiN_x produced by ion implantation in silicon. A clear difference in the XANES changes with the x value was found between oxide and nitride. XANES spectra at the Si $2p$ and Si $2s$ edges for SiO_x resemble those reported for SiO_2 even at $x = 0.2$, and those at O $1s$ are independent of the fluence. These observations suggest that the conduction band of the SiO_x is mainly composed of orbitals of SiO_2. On the other hand, the XANES spectrum for SiN_x changes with the x value, and the sharp resonance corresponding to N dangling bonds appears at the N $1s$ edge for $x \geq 1.1$. These findings imply that the Si_3N_4 phase of stoichiometric composition is a minor component, and each silicon atom is coordinated to nitrogen and silicon atoms with the probability statistically determined.

ACKNOWLEDGMENTS

The authors wish to thank Professor S. Suga and Dr. H. Daimon of Osaka University for their valuable discussions. The staff of the Photon Factory in the National Laboratory for High-Energy Physics are gratefully acknowledged for their support in the XANES measurements. This work has been performed under the approval of Photon Factory Program Advisory Committee (PF-PAC No. 91-276).

[1] *Silicon Nitride for Microelectronics Applications,* edited by J. T. Milek (IFI/Plenum, New York, 1971).
[2] *The Physics of SiO_2 and its Interfaces,* edited by S. T. Pantelides (Pergamon, New York, 1978).
[3] C. E. Morosanu, Thin Solid Films **65**, 171 (1980).
[4] *The Physics of MOS Insulators,* edited by G. Lucovsky, S. T. Pantelides, and F. L. Galeener (Pergamon, New York, 1980).
[5] M. J. Powell, B. C. Easton, and O. F. Hill, Appl. Phys. Lett. **38**, 794 (1981).
[6] M. J. Powell, Appl. Phys. Lett. **43**, 597 (1983).
[7] H. Daimon and Y. Murata, Jpn. J. Appl. Phys. **21**, L217 (1982).
[8] J. Finster, D. Schulze, and A. Meisel, Surf. Sci. **162**, 671 (1985).
[9] J. H. Thomas III and S. Hofmann, J. Vac. Sci. Technol. A **3**, 1921 (1985).
[10] M. J. O'Leary and J. H. Thomas III, J. Vac. Sci. Technol. A **5**, 106 (1987).
[11] F. Lutz, J. L. Bischoff, L. Kubler, and D. Bolmont, Phys. Rev. B **40**, 10 356 (1989).
[12] N. Aoto, E. Ikawa, N. Endo, and Y. Kurogi, Surf. Sci. **234**, 121 (1990).

[13]M. Niwano, H. Katakura, Y. Takeda, Y. Takakuwa, N. Miyamoto, A. Hiraiwa, and K. Yagi, J. Vac. Sci. Technol. A **9**, 195 (1991).
[14]R. Alfonsetti, L. Lozzi, M. Passacantando, P. Picozzi, and S. Santucci, Thin Solid Films **213**, 158 (1992).
[15]H. Yamamoto, Y. Baba, and T. A. Sasaki, J. Surf. Sci. Soc. Jpn. **13**, 310 (1992).
[16]H. Yamamoto, Y. Baba, and T. A. Sasaki, Nucl. Instrum. Methods Phys. Res. B **73**, 587 (1993).
[17]H. Yamamoto, Y. Baba, and T. A. Sasaki (unpublished).
[18]R. Kärcher, L. Ley, and R. L. Johnson, Phys. Rev. B **30**, 1896 (1984).
[19]Y. Baba, T. A. Sasaki, and I. Takano, J. Vac. Sci. Technol. A **6**, 2945 (1988).
[20]Y. Baba, T. A. Sasaki, and I. Takano, Surf. Sci. **221**, 609 (1989).
[21]O. A. Ershov and A. P. Lukirskii, Fiz. Tverd. Tela (Leningrad) **8**, 2137 (1966) [Sov. Phys. Solid State **8**, 1699 (1967)].
[22]C. Gahwiller and F. C. Brown, Phys. Rev. B **2**, 1918 (1970).
[23]F. C. Brown and O. P. Rustgi, Phys. Rev. Lett. **28**, 497 (1972).
[24]A. Bianconi, Surf. Sci. **89**, 41 (1979).
[25]A. Bianconi and R. S. Bauer, Surf. Sci. **99**, 76 (1980).
[26]T. Hattori, Y. Hisajima, H. Saito, T. Suzuki, H. Daimon, Y. Murata, and M. Tsukada, Appl. Phys. Lett. **42**, 244 (1983).
[27]E. O. Filatova, A. S. Vinogradov, and T. M. Zimkina, Fiz. Tverd. Tela (Leningrad) **27**, 997 (1985) [Sov. Phys. Solid State **27**, 606 (1985)].
[28]G. R. Harp, Z. L. Han, and B. P. Tonner, Phys. Scr. **T31**, 23 (1990).
[29]N. Niwano, Y. Takamura, H. Katakura, and N. Miyamoto, J. Vac. Sci. Technol. A **9**, 212 (1991).
[30]R. D. Leapman and L. A. Grunes, Phys. Rev. Lett. **45**, 397 (1980).
[31]R. D. Leapman, L. A. Grunes, and P. L. Fejes, Phys. Rev. B **26**, 614 (1982).
[32]H. Sekiyama, M. Nakazawa, and S. Kawase, Jpn. J. Appl. Phys. **29**, L141 (1990).
[33]R. J. Temkin, J. Non-Cryst. Solids **17**, 215 (1975).
[34]H. R. Philipp, J. Phys. Chem. Solids **32**, 1935 (1971).
[35]A. Knop, U. Dobler, E. C. Paloura, S. Logothetidis, and D. R. Batchelor (unpublished).
[36]E. C. Paloura, A. Knop, U. Dobler, K. Holldack and S. Logothetidis (unpublished).
[37]W. Warren, F. C. Fong, E. H. Poindexter, G. J. Gerardi, and J. Kanicki, J. Appl. Phys. **70**, 346 (1991).
[38]J. Robertson and M. J. Powell, Appl. Phys. Lett. **44**, 415 (1984).